Chapter 1

Exact Model for Single Atom Transistor

Er'el Granot

Additional information is available at the end of the chapter

http://dx.doi.org/10.5772/intechopen.70445

Abstract

An exact model for a single atom transistor was developed. Using two simplifying assumptions (1) that the device is restricted to a narrow conducting wire and (2) that the atom can be simulated by a point impurity potential, the model can be simplified considerably and an *exact analytical solution* can be derived. Thus, analytical solution is approximated to a close-form solution in three important regimes: at the vicinity of the resonance energy (near the maximum peak), at the vicinity of the inverse resonance, i.e., Fano resonance (near the minimum), and at the threshold energy where a universal transmission pattern appears. Finally, physical values are applied to demonstrate that this device can operate as a transistor, when it is calibrated to work at the vicinity of its maximum and minimum points.

Keywords: quantum dots, quantum point defect, point impurity, quantum transistor, single atom transistor

1. Introduction

In accordance with the rapid growth of calculation power, the transistor dimensions shrink exponentially. Surprisingly, more than 50 years after Gordon Moore made his observation in 1965 (or, more accurately, its revised form a decade later), that the number of transistors on a single chip doubles every couple of years, this observation is still valid [1, 2]. The number of transistors in a chip keeps growing despite the fact that the chip clock speed and its power consumption seem to be stagnated.

To meet the demands of the current trend, the average transistor size should decrease to the dimensions of a single atom, which is the smallest quantum dot, within about a decade.

The ability to move and manipulate single Xenon atoms (in Eigler and Schweizer lab at IBM's Almaden Research Center) in the early 1990s was a great leap in that direction [3].

In the attempts to meet this requirement, scientists already demonstrated the operation on several atoms and dopants [4–9] and even on single atoms [10–12]. The atom can be utilized as a stationary gate [10] or as a dynamic switch [13].

Such a device indeed consists of a single atom, but its conductor leads are of mesoscopic dimensions. Consequently, this is a complicated device to simulate and requires heavy software.

However, since the process is dominated by resonant tunneling, the model can be simplified considerably. In this case, only a single energy level of the quantum dot is relevant to the process, and therefore, it can be simulated by a point defect potential.

A point defect potential has a single eigen bound state, and therefore, it can simulate a quantum dot or a small atom in a relatively narrow spectral domain.

While a delta function can simulate a point defect in one-dimensional (1D) systems, a two-dimensional (2D) delta function cannot scatter and therefore cannot simulate a quantum dot. Azbel suggested to use an Impurity-D-Function (IDF) to simulate point defects in 2D quantum systems [14, 15] (for a comprehensive discussion and derivations, see Ref. [16]).

Several years later, the IDF was utilized in simulations of resonant tunneling through an opaque quantum barrier via a point defect in the presence [17] and absence [18] of a magnetic field. However, in these models, it was taken that there is a degeneracy in the y-direction, i.e., it was assumed that the barrier's transverse dimension is infinite and therefore cannot be applied in a system, where the current is carried by narrow wires (as in modern single atom transistor's devices).

On the other hand, conductance of nanowires with defects, but without a barrier, received lots of attention in the literature, exhibiting a wealth of physical phenomena [4–9, 19–21].

It is the purpose of this chapter to integrate the two, i.e., to formulate a model, which incorporates resonant tunneling via a point defect and wire conductance. That is, both the potential barrier and the impurity are located in the nanowire.

2. The model

The system is illustrated in **Figure 1**. It consists of two semi-infinite conducting wires, which are separated by an insulating gap. Within this gap, there is a quantum dot, which characterizes the resonance atom. To simplify the analysis, it is assumed that the wire boundaries in the y direction are totally reflecting, i.e., the wire is bounded by an infinitely large potential. Moreover, the single atom is modeled by a point defect potential.

It is also taken that this is a 2D model, i.e., there are no variations in the third dimension. This is a good approximation provided the wire is narrower in the z-dimension. Another advantage in constructing the model in 2D is that point impurities potential cannot exist in higher than two dimensions (see Ref. [16]).

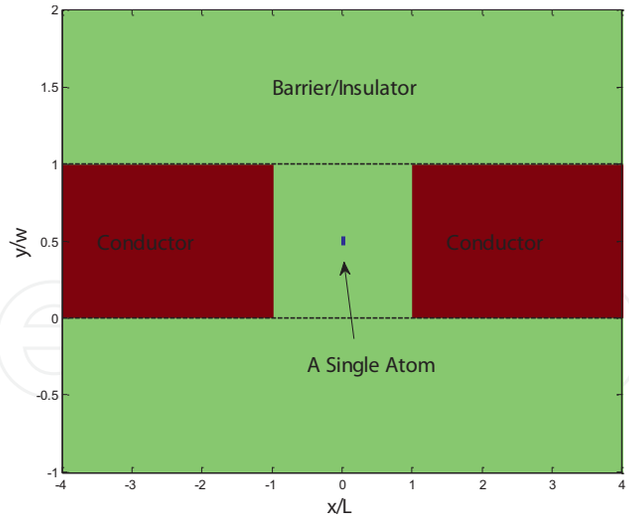

Figure 1. Model schematic.

Therefore, the system can be described by the following stationary Schrödinger equation

$$-\nabla^2\Psi(x,y) + [V(x) + U(y) - D(\mathbf{r}' - \mathbf{r}_0)]\Psi(x,y) = E\Psi(x,y) \tag{1}$$

in which normalized units (where Planck constant is $\hbar = 1$, and the electron's mass is $m = 1/2$) were used. In this equation,

$$U(y) = \begin{cases} 0 & 0 < y < w \\ \infty & else \end{cases} \tag{2}$$

is the boundaries' potential, which confines the dynamics to the wire geometry.

The potential of the gap between the wires is represented by the finite potential barrier,

$$V(x) = \begin{cases} V & |x| < L \\ 0 & else \end{cases} \tag{3}$$

and for the point impurity potential, we use an asymmetric Impurity D Functions (see Refs. [14, 15])

$$D(\mathbf{r}) = \lim_{\rho\to 0} \frac{2\sqrt{\pi}\,\exp\left(-y^2/\rho^2\right)}{\rho \ln\left(\rho_0/\rho\right)} \delta(x), \tag{4}$$

where $\mathbf{r} = \widehat{x}x + \widehat{y}y$, and the location of the point impurity is $\mathbf{r}_0 = \widehat{x}x_0 + \widehat{y}y_0$. ρ_0 is the de-Broglie wavelength of the impurity's bound eigenstate. The eigenenergy of the bound state of this impurity is

$$E_0 = -\frac{16\exp(-\gamma)}{\rho_0^2} \cong -\frac{8.98}{\rho_0^2} \tag{5}$$

where $\gamma \cong 0.577$ is Euler constant [22].

It should be stressed that this point impurity potential is an excellent approximation to a small quantum dot defect, i.e., a finite but small impurity, with a radius a and potential V_0 provided

$$\rho_0 = 2a \exp\left(\frac{2}{V_0 a^2} + \frac{\gamma}{2}\right). \tag{6}$$

3. Derivation of the exact analytical solution

The solution of Eq. (1) reads (see Refs. [16, 19])

$$\Psi(\mathbf{r}) = \Psi_{inc}(\mathbf{r}) - \frac{G^+(\mathbf{r}, \mathbf{r}_0)\Psi_{inc}(\mathbf{r}_0)}{1 + \int d\mathbf{r}' G^+(\mathbf{r}', \mathbf{r}_0) D(\mathbf{r}' - \mathbf{r}_0)} \int d\mathbf{r}' D(\mathbf{r}' - \mathbf{r}_0) \tag{7}$$

where $\Psi_{inc}(\mathbf{r})$ is the incoming wavefunction, $G^+(\mathbf{r}, \mathbf{r}_0)$ is the outgoing 2D Green function, i.e., $G^+(\mathbf{r}, \mathbf{r}_0)$ is the solution of the partial differential equation

$$-\nabla^2 G^+(\mathbf{r}, \mathbf{r}_0) + [V(x) + U(y) - E] G^+(\mathbf{r}, \mathbf{r}_0) = -\delta(\mathbf{r} - \mathbf{r}_0). \tag{8}$$

Both the incoming wavefunction $\psi_{inc}(\mathbf{r})$ and the Green function can be written as a superposition of the homogenous solution of Eq. (1) $\varphi^+_{m,E}(\mathbf{r})$, i.e., solution of the equation where the impurity is absent. These solutions are characterized by two quantum parameters: the energy E and the mode number m, namely

$$-\nabla^2 \phi^\pm_{m,E}(\mathbf{r}) + [V(x) + U(y) - E] \phi^\pm_{m,E}(\mathbf{r}) = 0 \tag{9}$$

where

$$\phi^\pm_{m,E}(\mathbf{r}) = \sqrt{\frac{2}{w}} \sin(m\pi y/w) \chi^\pm_{E,m}(x) \tag{10}$$

and $\chi^\pm_{E,m}(x)$ are the homogeneous solutions of the 1D equation

$$-\frac{\partial^2}{\partial x^2} \chi^\pm_{E,m}(x) + \left[V(x) + (m\pi/w)^2 - E\right] \chi^\pm_{E,m}(x) = 0, \tag{11}$$

where the superscript "+" and "−" stand for propagation to the right and to the left respectively.

Similarly, it is convenient to formulate the 2D Green function in terms of the 1D one $[G^+_{1D}(x, x'; E)]$:

$$G^+(\mathbf{r}, \mathbf{r}') = \frac{2}{w} \sum_{n=1}^{\infty} \sin(n\pi y/w) \sin(n\pi y'/w) G^+_{1D}(x, x'; E_n) \tag{12}$$

where $E_m \equiv E - (m\pi/w)^2$ and $G^+_{1D}(x, x'; E)$ solves the equation

$$-\frac{\partial^2}{\partial x^2} G^+_{1D}(x, x'; E_m) + [V(x) + E_m] G^+_{1D}(x, x'; E_m) = -\delta(x - x') \tag{13}$$

with the boundary condition

$$\frac{\partial}{\partial x} G^+_{1D}(x, x'; E_m) \mp i\sqrt{E_m} G^+_{1D}(x, x'; E_m) = 0 \,\text{for}\, x \to \pm\infty. \tag{14}$$

Therefore,

$$G^+_{1D}(x, x'; E_m) = \begin{cases} \dfrac{\chi^{\pm}_{E,m}(x)/\chi^{\pm}_{E,m}(x_0)}{\chi^{\pm}_{E,m}{}'(x)/\chi^{\pm}_{E,m}(x_0) - \chi^{\pm}_{E,m}{}'(-x)/\chi^{\pm}_{E,m}(-x_0)} & x > x_0 \\ \dfrac{\chi^{\pm}_{E,m}(-x)/\chi^{\pm}_{E,m}(-x_0)}{\chi^{\pm}_{E,m}{}'(x)/\chi^{\pm}_{E,m}(x_0) - \chi^{\pm}_{E,m}{}'(-x)/\chi^{\pm}_{E,m}(-x_0)} & x < x_0 \end{cases} \tag{15}$$

where the tags stand for spatial derivatives.

In the case of a rectangular barrier (in a slightly different writing, see Ref. [23])

$$\chi^+_{k,n}(x) = \begin{cases} \exp(ik_n x) + t_n R_n \exp(-ik_n x) & x < -L \\ t_n C_n \exp(-K_n x) + t_n D_n \exp(K_n x) & |x| < L \\ t_n \exp(ik_n x) & x > L \end{cases} \tag{16}$$

where

$k_m \equiv \sqrt{E_m} = \sqrt{E - (m\pi/w)^2}$ and $K_m \equiv \sqrt{V - E_m} = \sqrt{V - E + (m\pi/w)^2}$;

$$\begin{aligned} t_n &= \frac{\exp(-2ik_n L)}{\cosh(2K_n L) + i(K_n/k_n - k_n/K_n)\sinh(2K_n L)/2} \\ &\cong 2\frac{\exp(-2ik_n L - 2K_n L)}{1 + i(K_n/k_n - k_n/K_n)/2}, \end{aligned} \tag{17}$$

$$C_n = \frac{1}{2}\left(1 - \frac{ik_n}{K_n}\right)\exp(K_n L + ik_n L), \tag{18}$$

$$D_n = \frac{1}{2}\left(1 + \frac{ik_n}{K_n}\right)\exp(-K_n L + ik_n L) \tag{19}$$

and

$$R_n = -\frac{i}{2}\left(\frac{K_n}{k_n} + \frac{k_n}{K_n}\right)\sinh(2K_n L). \tag{20}$$

The general Green function is then

$$G_{1D}^{+}(x,x_0;E_m) \cong \frac{1}{M_n}\begin{cases} \dfrac{\exp(ik_n x)}{C_n\exp(-K_n x_0)+D_n\exp(K_n x_0)} & L<x \\ \dfrac{C_n\exp(-K_n x)+D_n\exp(K_n x)}{C_n\exp(-K_n x_0)+D_n\exp(K_n x_0)} & x_0<x<L \\ \dfrac{C_n\exp(K_n x)+D_n\exp(-K_n x)}{C_n\exp(K_n x_0)+D_n\exp(-K_n x_0)} & -L<x<x_0 \\ \dfrac{\exp(-ik_n x)}{C_n\exp(K_n x_0)+D_n\exp(-K_n x_0)} & x<-L \end{cases} \tag{21}$$

where

$$M_n = -K_n[\tanh[K_n(L-x_0)+i\theta(k_n)]+\tanh[K_n(L+x_0)+i\theta(k_n)]]$$

and then

$$G_{1D}^{+}(x,x_0;E_m) = \frac{\frac{\tanh[K_m(L-x)+i\theta(k_m)]}{\tanh[K_m(L-x_0)+i\theta(k_m)]}}{-K_m[\tanh[K_m(L-x_0)+i\theta(k_m)]+\tanh[K_m(L+x_0)+i\theta(k_m)]]} \text{ for } |x|<L \tag{22}$$

using

$$\tan\theta(k) = -k/K. \tag{23}$$

Then

$$\begin{aligned} G_{1D}^{+}(x_0,x_0;E_m) &= \frac{1}{-K_m[\tanh[K_m(L-x_0)+i\theta(k_m)]+\tanh[K_m(L+x_0)+i\theta(k_m)]]} \\ &\cong \frac{1}{-2K_m\left[1-2\exp[-2K_mL-2i\theta(k_m)]\cosh[2K_mx_0]\right]} \end{aligned} \tag{24}$$

where the last term is an approximation in the limit of opaque barriers.

When the incoming wavefunction is the mth mode

$$\Psi_{inc}(\mathbf{r}) = \sin\left(\frac{m\pi y}{w}\right)\chi_{E,m}^{+}(x) \tag{25}$$

then, the solution (in all space) reads

$$\begin{aligned} \Psi(\mathbf{r}) = {} & \sin\left(\frac{m\pi y}{w}\right)\chi_{E,m}^{+}(x) \\ & + \frac{\sin\left(\frac{m\pi y_0}{w}\right)\chi_{E,m}^{+}(x_0)\frac{2}{w}\sum_{n=1}^{\infty}\sin\left(\frac{n\pi y}{w}\right)\sin\left(\frac{n\pi y_0}{w}\right)G_{1D}^{+}(x,x_0;E_n)}{\frac{1}{2\pi}\ln\left(\frac{\rho_0}{\rho}\right)+\frac{2}{w}\sum_{n=1}^{\infty}\sin^2\left(\frac{n\pi y_0}{w}\right)G_{1D}^{+}(x_0,x_0;E_n)\exp\left(-\left(\frac{n\pi\rho}{2w}\right)^2\right)} \end{aligned} \tag{26}$$

which can be written as

$$\Psi(x>L,y)=\sum_{p}\sin\left(\frac{p\pi y}{w}\right)\chi^{+}_{E,p}(x)$$
$$\times\left\{\delta(p-m)-\frac{\sin\left(\frac{m\pi y_0}{w}\right)\sin\left(\frac{p\pi y_0}{w}\right)\frac{\chi^{+}_{E,m}(x_0)}{\chi^{+}_{E,p}(x_0)}\frac{2}{w}G^{+}_{1D}(x_0,x_0;E_p)}{\frac{1}{2\pi}\ln\left(\frac{\rho_0}{\rho}\right)+\frac{2}{w}\sum_{n=1}^{\infty}\sin^2\left(\frac{n\pi y_0}{w}\right)G^{+}_{1D}(x_0,x_0;E_n)\exp\left(-\left(\frac{n\pi\rho}{2w}\right)^2\right)}\right\}. \tag{27}$$

In the case where the incoming particle's energy satisfies

$$(\pi/w)^2<E<(2\pi/w)^2$$

then only a single mode propagates, in which case

$$\Psi(x\to\infty,y)=\sin\left(\frac{\pi y}{w}\right)\chi^{+}_{E,1}(x)t_{11} \tag{28}$$

where t_{11} is the transmission coefficient to remain at $x\to\infty$ in the first mode, which is

$$t_{11}\equiv 1-\frac{\sin^2\left(\frac{\pi y_0}{w}\right)\frac{2}{w}G^{+}_{1D}(x_0,x_0;E_1)}{\frac{1}{2\pi}\ln\left(\frac{\rho_0}{\rho}\right)+\frac{2}{w}\sum_{n=1}^{\infty}\sin^2\left(\frac{n\pi y_0}{w}\right)G^{+}_{1D}(x_0,x_0;E_n)\exp\left(-\left(\frac{n\pi\rho}{2w}\right)^2\right)} \tag{29}$$

A plot of $T_{11}=|t_{11}|^2$ as a function of the incoming particle's energy is presented in **Figure 2**.

Clearly, a resonance occurs when the real part of the denominator of Eq. (29) vanishes, i.e. when

$$\frac{1}{2\pi}\ln\left(\frac{\rho_0}{\rho}\right)+\frac{2}{w}\sum_{n=1}^{\infty}\sin^2\left(\frac{n\pi y_0}{w}\right)\Re G^{+}_{1D}(x_0,x_0;E_n)\exp\left(-\left(\frac{n\pi\rho}{2w}\right)^2\right)=0. \tag{30}$$

In general, it is a complex transcendental equation; however, in case of an opaque barrier, Eq. (24) can be further simplified to

$$G_{1D}(x_0,x_0;E_n)\cong-\frac{1}{2K_n}+i\varepsilon_n \tag{31}$$

when

$$\varepsilon_n\equiv\frac{\exp[-2K_nL]\sin[2\theta(k_n)]\cosh(2K_nx_0)}{K_n}=-2\frac{\exp[-2K_nL]k_n\cosh(2K_nx_0)}{V}, \tag{32}$$

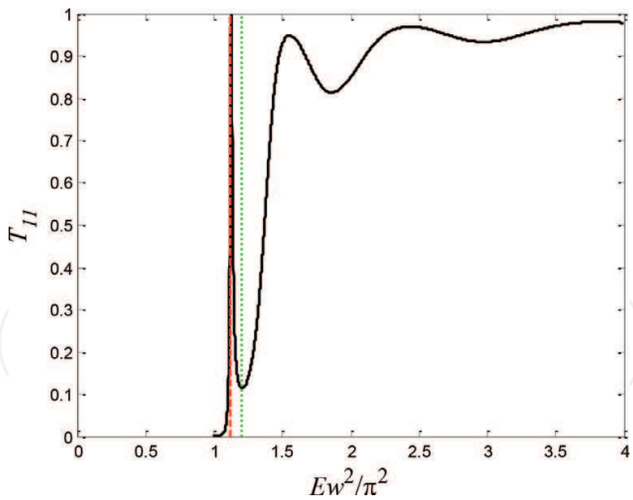

Figure 2. Plot of the $T_{11} = |t_{11}|^2$, i.e., the probability to remain in the first mode of propagation as a function of the normalized energy. The barrier parameters were $L = 2w$ and $V = 2/w^2$, and the defect parameters were $\rho_0 = 300w$, $x_0 = 0$, and $y_0 = w/2$. The dotted line represents the barrier's energy $E_b = V + \pi^2/w^2$, and the dashed line represents the resonance energy E_{res}.

$$\text{and } \sin\left[2\theta(k_1)\right] = \frac{-2kK}{K^2 + k^2} = \frac{-2kK}{V}. \tag{33}$$

Then, Eq. (30) can be approximated as

$$\frac{1}{2\pi}\ln\left(\frac{\rho_0}{\rho}\right) - \frac{2}{w}\sum_{n=1}^{\infty}\sin^2\left(\frac{n\pi y_0}{w}\right)\frac{1}{2K_n}\exp\left(-\left(\frac{n\pi\rho}{2w}\right)^2\right) = 0 \tag{34}$$

In the case where the conducting wires is very narrow or the barrier is very high, i.e.,

$$(\pi/w)^2 + V >> E_0 \tag{35}$$

then

$$\frac{1}{2\pi}\ln\left(\frac{\rho_0}{\rho}\right) - \frac{1}{w}\sin^2\left(\frac{\pi y_0}{w}\right)\frac{1}{\sqrt{V - E + (\pi/w)^2}} - \frac{1}{\pi}\sum_{n=2}^{\infty}\sin^2\left(\frac{n\pi y_0}{w}\right)\frac{1}{\sqrt{n^2-1}}\exp\left(-\left(\frac{n\pi\rho}{2w}\right)^2\right) = 0 \tag{36}$$

since

$$\sum_{n=2}^{\infty}\sin^2\left(\frac{n\pi y_0}{w}\right)\frac{1}{\pi\sqrt{n^2-1}}\exp\left(-\left(\frac{n\pi\rho}{2w}\right)^2\right) \cong -\ln(4\rho/w)/2\pi \tag{37}$$

then

$$\frac{1}{2\pi}\ln\left(\frac{4\rho_0}{w}\right) = \frac{1}{w}\sin^2\left(\frac{\pi y_0}{w}\right)\frac{1}{\sqrt{V - E + (\pi/w)^2}} \tag{38}$$

which has a solution provided $4\rho_0 > w$, otherwise the impurity can be regarded as a perturbation and does not carry a resonant level.

When the resonant level exits, then the resonance energy E_R is approximately

$$E_R \cong V + \frac{\pi^2}{w^2}\left\{1 - \sin^4\left(\frac{\pi y_0}{w}\right)\left[\frac{1}{2}\ln\left(\frac{4\rho_0}{w}\right)\right]^{-2}\right\} \tag{39}$$

In **Figure 2**, the resonance energy is presented by a dashed line.

In this approximation,

$$\Psi(\mathbf{r}) \cong \sin\left(\frac{\pi y}{w}\right)\chi^{+}_{E,1}(x)\frac{1}{K_1\frac{w}{2\pi}\ln\left(\frac{4\rho_0}{w}\right)/\sin^2\left(\frac{\pi y_0}{w}\right) - (1 + i2K_1\varepsilon_n)} \tag{40}$$

Since in this regime only, one transverse mode is propagating, the system in practice reduces to a 1D problem, where the 2D impurity can be replaced by a 1D delta function potential

$$V(x) = -\lambda\delta(x) \tag{41}$$

where

$$\lambda = \frac{4\pi}{w\ln(4\rho_0/w)}\sin^2\left(\frac{\pi y_0}{w}\right). \tag{42}$$

Therefore, in the 1D analogy the point potential depends not only on the impurity's de-Broglie wavelength in free space, but on its location (y_0) and the wire's width as well.

In this case, the barrier's transmission can be as high as 1. It depends on the location of the point defect in the horizontal dimension, namely, at the resonance energy

$$\Psi(\mathbf{r}) = i\sin\left(\frac{\pi y}{w}\right)\exp(ik_1x)\frac{\exp(-2ik_1L + i\Xi)}{\cosh(2K_1x_0)} \tag{43}$$

where

$$\tan\Xi = -(K/k - k/K)/2. \tag{44}$$

However, there is a point where a minimum occurs. When the incoming particle's energy satisfies

$$\frac{1}{2\pi}\ln\left(\frac{\rho_0}{\rho}\right) + \frac{2}{w}\sum_{n=2}^{\infty}\sin^2\left(\frac{n\pi y_0}{w}\right)\Re G^{+}_{1D}(x_0, x_0; E_n)\exp\left(-\left(\frac{n\pi\rho}{2w}\right)^2\right) = 0 \tag{45}$$

which at the vicinity of the second mode threshold can be approximated by

$$\frac{1}{2\pi}\ln\left(\frac{\rho_0}{\rho}\right)-\frac{1}{w}\sin^2\left(\frac{2\pi y_0}{w}\right)\frac{1}{\sqrt{V-E+(2\pi/w)^2}}-\frac{1}{\pi}\sum_{n=3}^{\infty}\sin^2\left(\frac{n\pi y_0}{w}\right)\frac{1}{\sqrt{n^2-4}}\exp\left(-\left(\frac{n\pi\rho}{2w}\right)^2\right)=0 \quad (46)$$

or

$$\frac{1}{2\pi}\ln\left(\frac{3.8\rho_0}{w}\right)=\frac{1}{w}\sin^2\left(\frac{2\pi y_0}{w}\right)\frac{1}{\sqrt{V-E+(2\pi/w)^2}}. \quad (47)$$

Again, we see that this equation does not always have a solution. It is required that $3.8\rho_0 > w$, in which case

$$E_{\min}=V+\left(\frac{2\pi}{w}\right)^2\left[1-\sin^4\left(\frac{2\pi y_0}{w}\right)\left[\ln\left(\frac{3.8\rho_0}{w}\right)\right]^{-2}\right] \quad (48)$$

This minimum is presented in **Figure 3** by a dotted line.

In which case, the denominator of Eq. (29) is exactly $\sin^2\left(\frac{\pi y_0}{w}\right)\frac{2}{w}G_{1D}^{+}(x_0,x_0;E_1)$, and therefore at this point, the transmission is exponentially small, and not zero as in the zero potential case, i.e.,

$$\begin{aligned}\Psi_{\min}(\mathbf{r}) &= \sin\left(\frac{\pi y}{w}\right)\chi_{E,1}^{+}(x)i\frac{\sin^2\left(2\pi y_0/w\right)}{\sin^2\left(\pi y_0/w\right)}\frac{\Im G_{1D}^{+}(x_0,x_0;E_2)}{\Re G_{1D}^{+}(x_0,x_0;E_1)}\\ &= -\sin\left(\frac{\pi y}{w}\right)\chi_{E,1}^{+}(x)i\frac{\sin^2\left(2\pi y_0/w\right)}{\sin^2\left(\pi y_0/w\right)}2K_1\varepsilon_2\end{aligned} \quad (49)$$

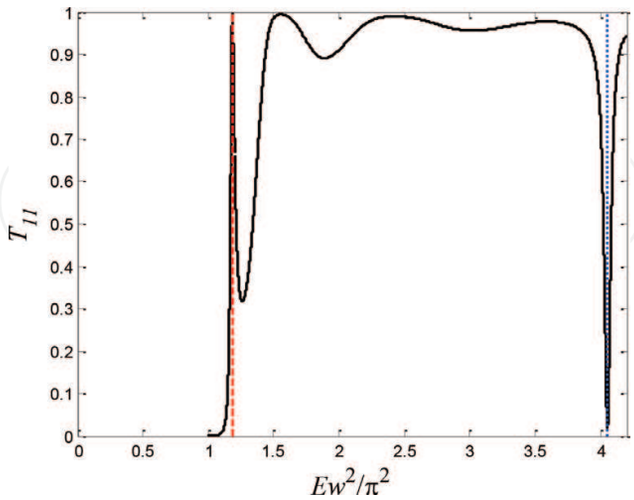

Figure 3. Plot of $T_{11} = |t_{11}|^2$, i.e., the probability to remain in the base (1) mode of propagation as a function of the normalized energy. The barrier parameters were $L = 2w$ and $V = 2/w^2$, and the defect parameters were $\rho_0 = 30w$, $x_0 = 0$, and $y_0 = 0.2w$. The dotted line represents the minimum transmission point $E_{\min}$, and the dashed line represents the resonance energy E_{res}.

which is an exponentially small value. This result agrees with Ref. [24].

It should be stressed, however, that this is a pure 2D phenomenon, which is a consequence of the interaction between the point defect and the wire, and therefore, this minimum disappears in the 1D approximation.

In **Figures 4–9**, a 2D probability density plots (of $|\psi(x, y)|^2$) for various energies are presented.

In **Figure 4**, the energy is too low for the particles to penetrate the barrier, and therefore, almost all of them are reflected from the barrier.

In **Figure 5**, the particle's energy is close to the resonance energy, and therefore, a quasi-bound state is generated at the vicinity of the defect, and the transmission probability is high.

Figures 6 and **7** are examples for local minimum and local maximum respectively.

In **Figure 8**, the particle's energy is close to the minimum (Eq. (48)), which was generated by the interplay between the waveguide and the point defect.

Another important working point is when $K_p = 0$, i.e., $V - E + (p\pi/w)^2 = 0$ and $k_p = \sqrt{V}$.

At this energy, a universal behavior appears. The scattered wavefunction reads

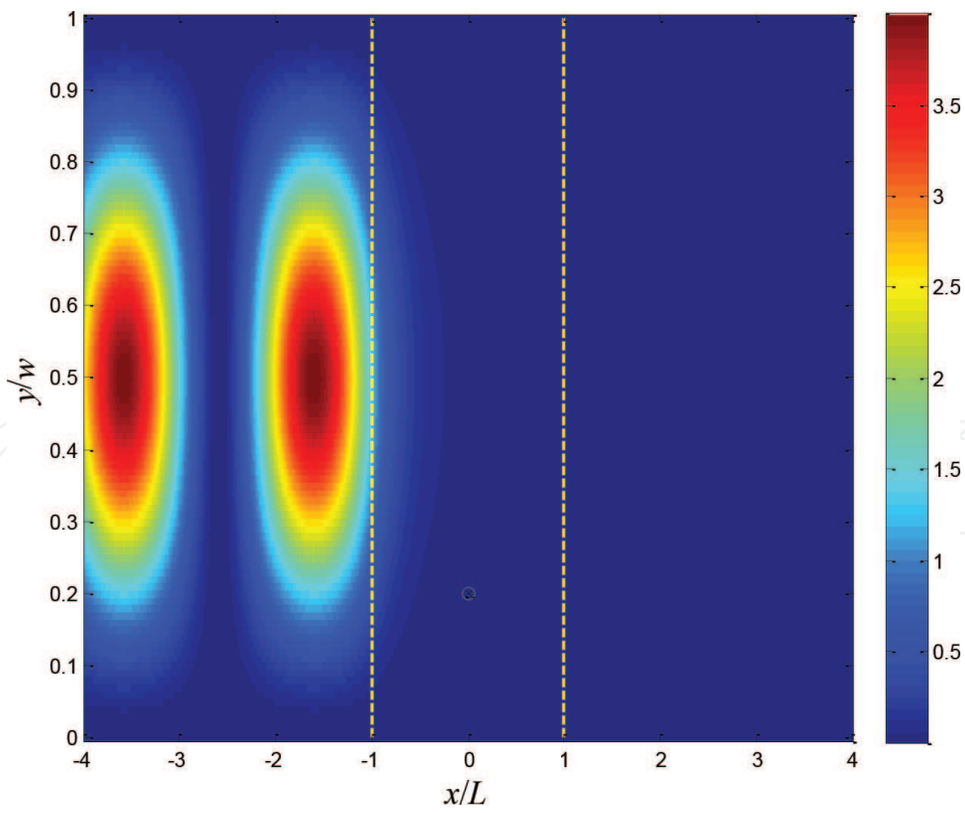

Figure 4. A false colors presentation of the probability density $|\Psi(x, y)|^2$ when the incoming particle's energy is lower than the barrier's height: $E = 10.5w^{-2} < (\pi/w)^2 + V \cong 11.87w^{-2}$. The parameters are same as in **Figure 3**. The dashed lines represent the barrier's boundaries, and the cross at the center of the circle represents the impurity's location.

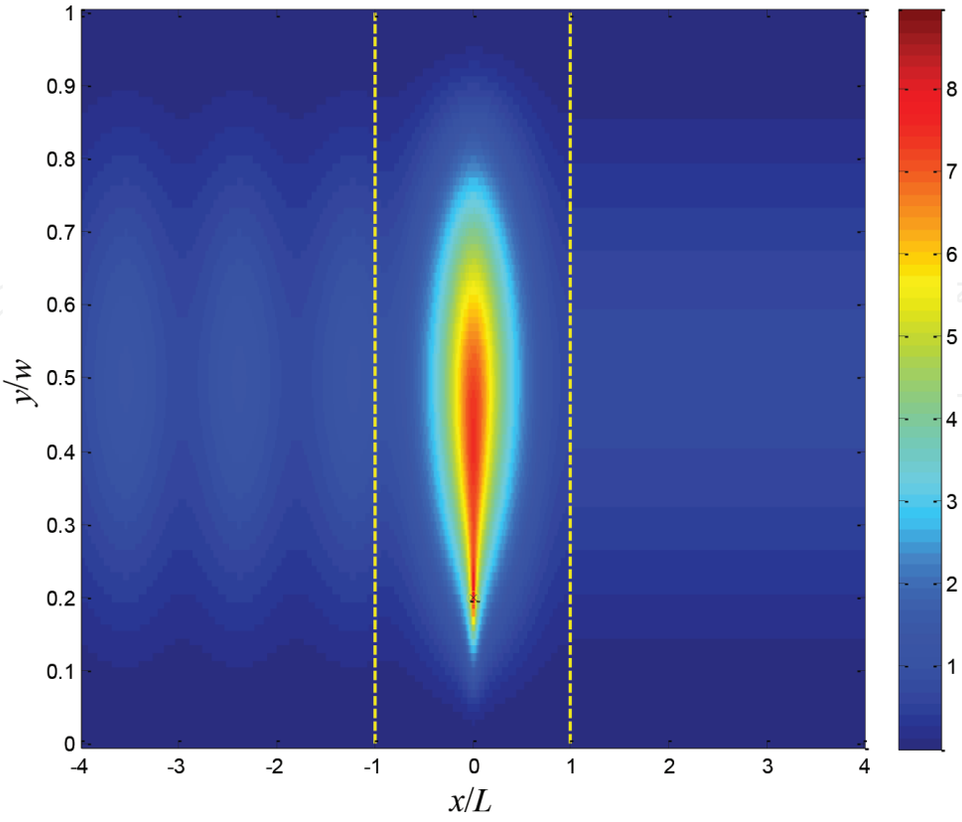

Figure 5. Same as **Figure 4** but when the income particle's energy is close to the resonance energy, i.e. $E = 11.69w^{-2} \cong E_{res}$.

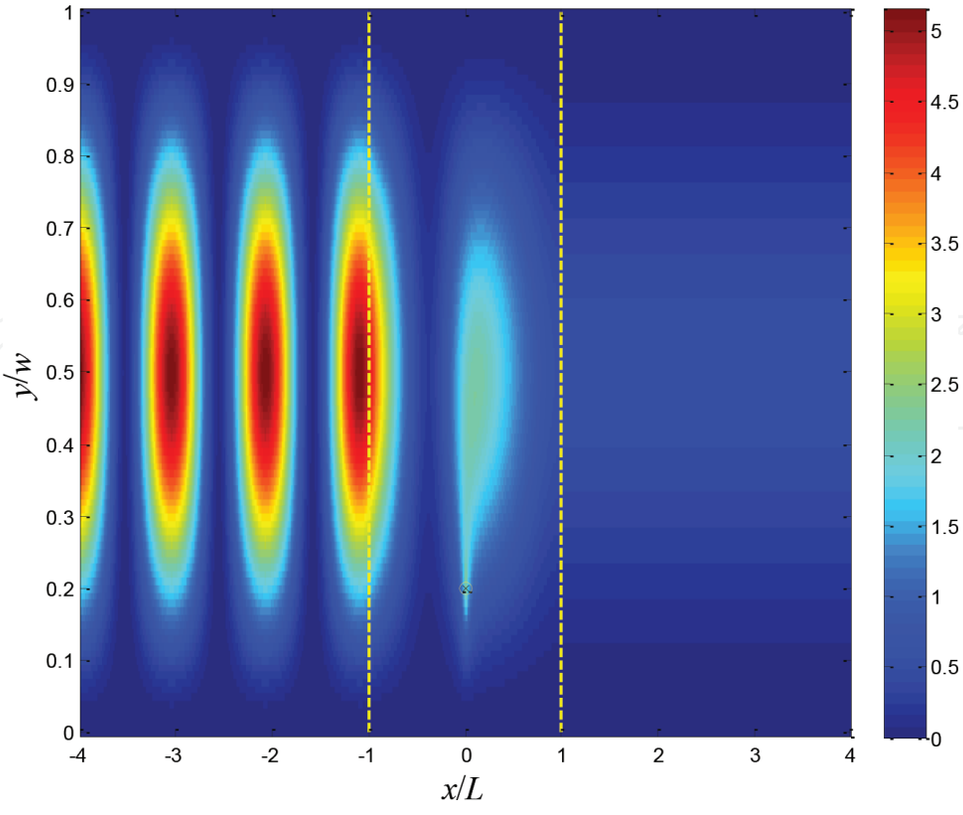

Figure 6. Same as **Figure 4** but when the income particle's energy is close to a local minimum at $E = 12.45w^{-2}$.

http://dx.doi.org/10.5772/intechopen.70445

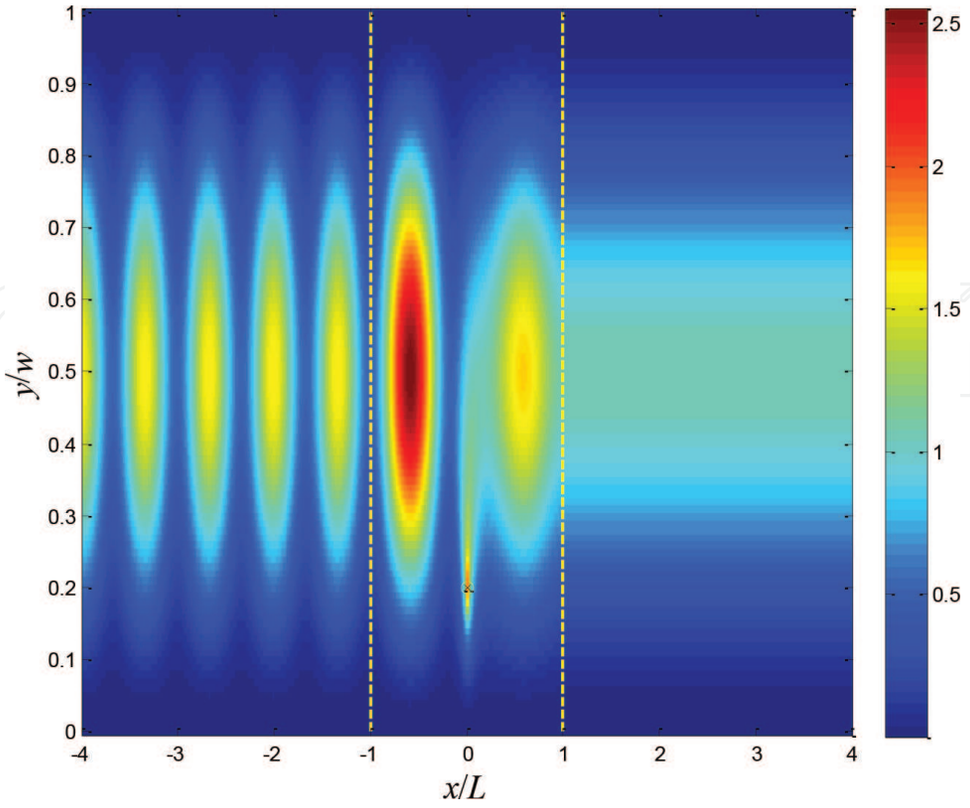

Figure 7. Same as **Figure 4** but when the income particle's energy is close to a local maximum at $E = 15.4w^{-2}$.

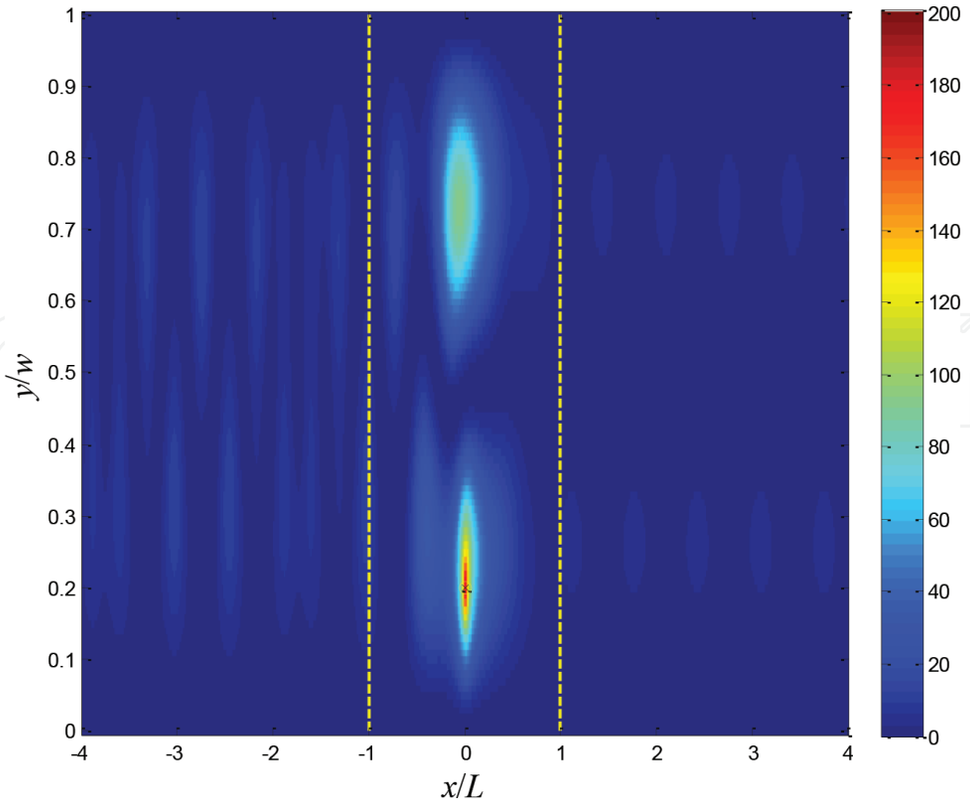

Figure 8. Same as **Figure 4** but when the income particle's energy is close to a local minima at $E = 40.02w^{-2}$.

$$\Psi(\mathbf{r}) = \sin\left(\frac{m\pi y}{w}\right)\chi^{+}_{E,m}(x) + \frac{\sin\left(\frac{m\pi y_0}{w}\right)\chi^{+}_{E,m}(x_0)\sin\left(\frac{p\pi y}{w}\right)G^{+}_{1D}(x,x_0;E_p)}{\sin\left(\frac{p\pi y_0}{w}\right)G^{+}_{1D}(x_0,x_0;E_p)}. \tag{50}$$

This expression is universal in the sense that it is independent of the point defect potential. It depends only on its location. In case this is a surface defect, i.e., $y_0/w << 1$ then even the dependence on the vertical location vanishes

$$\Psi(\mathbf{r}) = \sin\left(\frac{m\pi y}{w}\right)\chi^{+}_{E,m}(x) + \frac{m}{p}\chi^{+}_{E,m}(x_0)\sin\left(\frac{p\pi y}{w}\right)\frac{G^{+}_{1D}(x,x_0;E_p)}{G^{+}_{1D}(x_0,x_0;E_p)}. \tag{51}$$

This universality agree with Ref. [25].

For $|x| < L$ Eq. (51) reduces to the simple form

$$\Psi(|x| < L, y) = \sin\left(\frac{m\pi y}{w}\right)\chi^{+}_{E,m}(x) + \frac{\sin\left(\frac{m\pi y_0}{w}\right)}{\sin\left(\frac{p\pi y_0}{w}\right)}\chi^{+}_{E,m}(x_0)\sin\left(\frac{p\pi y}{w}\right) \tag{52}$$

and in the case of a surface defect, it reduces to even a simpler expression

$$\Psi(|x| < L, y) = \sin\left(\frac{m\pi y}{w}\right)\chi^{+}_{E,m}(x) + \frac{m}{p}\chi^{+}_{E,m}(x_0)\sin\left(\frac{p\pi y}{w}\right) \tag{53}$$

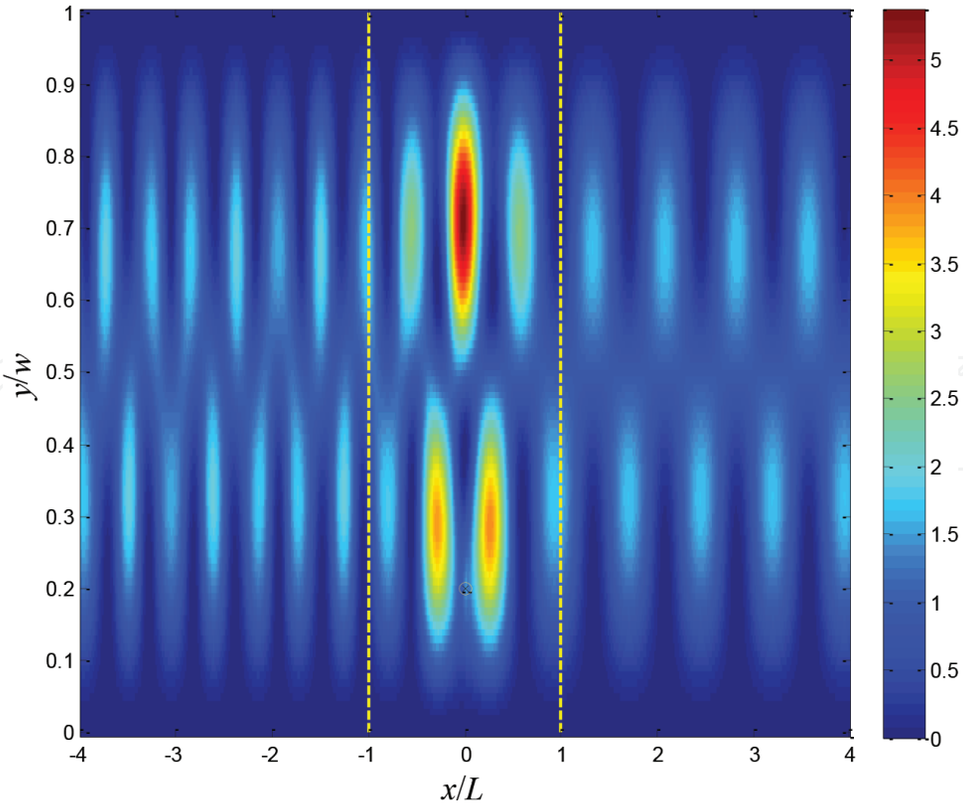

Figure 9. At the transition level $E = V + (\pi/w)^2$, a universal pattern appears.

The fact that the second part is independent of x is also in agreement with Ref. [25].

But unlike Ref. [25], due the barrier, the second mode does propagate, but the expression is still generic (in the sense that it is independent of the impurity's parameter), beyond the barrier it reads

$$\Psi(|x| > L, y) = \sin\left(\frac{m\pi y}{w}\right)\chi^{+}_{E,m}(x) + \frac{m}{p}\chi^{+}_{E,m}(x_0)\sin\left(\frac{p\pi y}{w}\right)\exp\left(i\sqrt{V}(|x| - L)\right). \tag{54}$$

This special universal case is illustrated in **Figure 9**, and it is a manifestation of the effect of Ref. [25], where the footprints of the defect are clearly seen but without any fingerprints. That is, the defect is clearly there, but the scattering is independent of its strength (its eigenenergy).

4. Physical realization and implementation

Let us apply this model to a 1.5-nm wide silicon wire, which is contaminated by a single phosphorous atom. In this case $w = 1.5$ nm, the phosphorous atom radius is $a = 0.098$ nm, the effective electron mass in silicon is $m_e \cong 0.2m$. Then the wire transmission (proportional to the device's conductivity in units of e^2/h) as a function of the potential at the atom's center V_0, Eq. (6) (which is proportional to the transistor gate voltage) is plotted in **Figure 10** for two scenarios. In the first scenario, the electron's energy, i.e., the Fermi energy, is $E = 0.9$ eV and in the second, it is equal to $E = 3$ eV. In the former scenario, the device works at the vicinity of the quantum dot's resonance, and in the latter, it works at the vicinity of the fano-(anti) resonance.

In both scenarios, a change of about a volt in the gate voltage can change drastically the wire's current. Therefore, it can be implemented as a simplified but rich model for a single atom transistor.

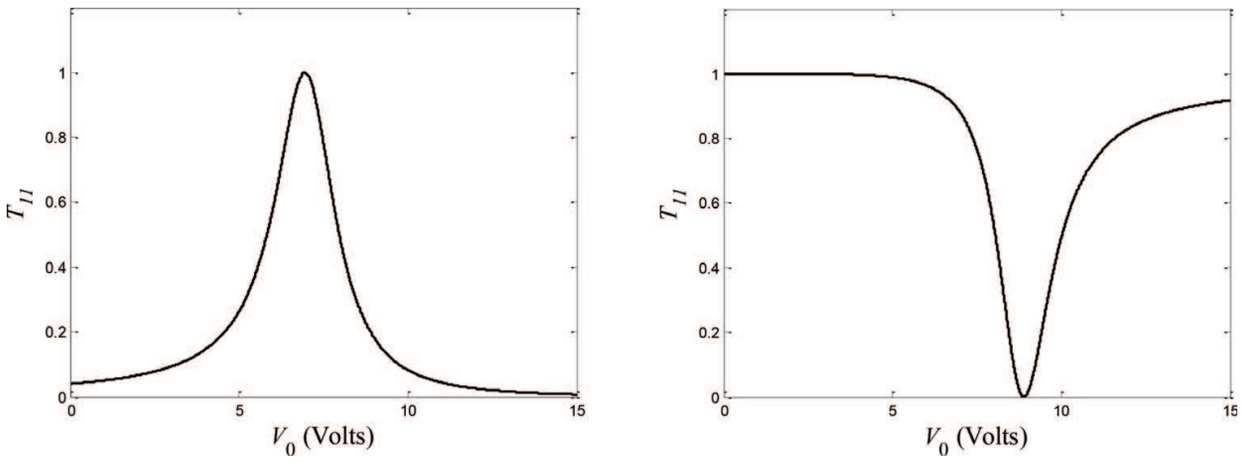

Figure 10. The wire's transmission as a function of the potential on the atom. In the left plot, the electron energy is $E = 0.9$ eV and in the right plot, $E = 3$ eV. The other parameters are $w = 1.5$ nm, $m_e \cong 0.2m$, $a = 0.098$ nm, $L = 2w = 3$ nm, and the potential barrier $V = 0.15$ eV.

Author details

Er'el Granot

Address all correspondence to: erel@ariel.ac.il

Department of Electrical and Electronics Engineering, Ariel University, Ariel, Israel

References

[1] Moore G. Chapter 7: Moore's law at 40. In: Brock D, editor. Understanding Moore's Law: Four Decades of Innovation. Philadelphia, PA: Chemical Heritage Foundation; 2006. pp. 67-84

[2] Takahashi D. Forty Years of Moore's Law. San Jose, CA: Seattle Times; April 18, 2005

[3] Eigler DM, Schweizer EK. Positioning single atoms with a scanning tunnelling microscope. Nature. 1990;**344**:524-526

[4] Koenraad PM, Flatté ME. Single dopants in semiconductors. Nature Materials. 2011;**10**: 91-100

[5] Lansbergen GP, et al. Gate-induced quantum-confinement transition of a single dopant atom in a silicon FinFET. Nature Physics. 2008;**4**:656-661

[6] Calvet LE, Snyder JP, Wernsdorfer W. Excited-state spectroscopy of single Pt atoms in Si. Physical Review B. 2008;**78**:195309

[7] Tan KY, et al. Transport spectroscopy of single phosphorus donors in a silicon nanoscale transistor. Nano Letters. 2010;**10**:11-15

[8] Hollenberg LCL, et al. Charge-based quantum computing using single donors in semiconductors. Physical Review B. 2004;**69**:113301

[9] Schofield SR, et al. Atomically precise placement of single dopants in Si. Physical Review Letters. 2003;**91**:136104

[10] Fuechsle M, Miwa JA, Mahapatra S, Ryu H, Lee S, Warschkow O, Hollenberg LCL, Klimeck G, Simmons MY. A single-atom transistor. Nature Nanotechnology. 2012;**7**:242-246

[11] Xie F-Q, Maul R, Wenzel W, Schn G, Obermair Ch, Schimmel Th. Single-atom transistors: Atomic-scale electronic devices in experiment and simulation. In: International Beilstein Symposium on Functional Nanoscience; Frankfurt am Main, May 2010. pp. 213-228

[12] Fuechsle M, Miwa JA, Mahapatra S, Warschkow O, Hollenberg LCL, Simmons MY. Realisation of a single-atom transistor in silicon. Journal and Proceedings of the Royal Society of New South Wales. 2012;**145**(443 & 444):66-74

[13] Obermair Ch, Xie F-Q, Schimmel Th. The single-atom transistor: Perspectives for quantum electronics on the atomic-scale. Europhysics News. 2010;**41**:25-28

[14] Azbel MY. Variable-range-hopping magnetoresistance. Physical Review B. 1991;**43**:2435

[15] Azbel MY. Quantum particle in a random potential: Implications of an exact solution. Physical Review Letters. 1991;**67**:1787

[16] Granot E. Point scatterers and resonances in low number of dimensions. Physica E. 2006;**31**:13-16

[17] Granot E, Azbel MY. Resonant angular dependence in a weak magnetic field. Journal of Physics: Condensed Matter. 1999;**11**:4031

[18] Granot E, Azbel MY. Resonant tunneling in two dimensions via an impurity. Physical Review B. 1994;**50**:8868

[19] Granot E. Near-threshold-energy conductance of a thin wire. Physical Review B. 1999;**60**:10664

[20] Granot E. Symmetry breaking and current patterns due to a weak imperfection. Physical Review B. 2000;**61**:11078

[21] Weber B, Mahapatra S, Ryu H, Lee S, Fuhrer A, Reusch TCG, Thompson DL, Lee WCT, Klimeck G, Hollenberg LCL, Simmons MY. Ohm's law survives to the atomic scale. Science. 2012;**335**:64

[22] Abramowitz M, Stegun IA. Handbook of Mathematical Functions. New York: Dover Publications; 1972

[23] Merzbacher E. Quantum Mechanics. Hoboken, NJ: Wiley; 1970

[24] Granot E. Universal conductance reduction in a quantum wire. Europhysics Letters. 2004;**68**:860-866

[25] Granot E. Transmission coefficient for a point scatterer at specific energies is affected by the presence of the scatterer but independent of the scatterer's characteristics. Physical Review B. 2005;**71**:035407

IntechOpen